

*XVII IMEKO World Congress  
Metrology in 3rd Millennium  
June 22-27, 2003, Dubrovnik, Croatia*

## **MODIFICATION OF RESONANCE CHARACTERISTICS OF ULTRASONIC TRANSDUCERS BY THE DRIVING CIRCUIT**

*Ch. Papageorgiou and Th. Laopoulos*

Electronics Lab. Physics Dept., Aristotle University of Thessaloniki,  
Thessaloniki, 54124, Greece

**Abstract** – A study of the resonance characteristics of low frequency ultrasonic transducers is presented in this work. The effect of the influence of the equivalent output resistance of the driving circuits on the shape of the frequency response and the sensitivity of the transducer is investigated. Theoretical presentation is accompanied by simulation analysis and verifying experimental measurements.

**Keywords:** ultrasonic transducers, resonance circuits, frequency response.

### 1. INTRODUCTION

In most applications of ultrasonic systems, the overall performance is strongly depended on the operational characteristics of the transducers, namely the frequency response curve and the sensitivity. The acoustic response of these devices depends rather significantly on the characteristics of the driving circuits, which provide the electrical connection of transducer to the electronic system. The amplitude, time duration, and shape of the transmitting pulses are affected by the front-end electronics of the system, leading thus to a situation where a different analysis should be performed depending on the specific application. Hence it is necessary to investigate the problem of the influence of these circuits on the frequency response (mainly) in order to design proper driving circuits for each case.

The currently accepted models of transducers can be ranged into two categories:

a) Very accurate models used for very accurate calculations of the behaviour of the transducers at different conditions. This category is mostly used for the design and development of transducers. The model in this case is the set of differential equations (differential equations with partial derivatives) that describe the behaviour of the transducer, together with the map of a grid that separates the body of the transducer into a multitude of elementary areas. These equations are solved numerically using this map with the help of a computer (something like SPICE), to produce the results of the transducer's behaviour. This technique is known as Finite Element Analysis. This method is time and memory-consuming and can be used to evaluate only a single transducer's behaviour. The evaluation of the

behaviour of complicated systems with two transducers, electronics and simple or complicated media of propagation is practically impossible, or requires extreme computing power.

b) The second category includes analytical models and equivalent circuits. These models are used for analytical calculations and simulations of complex systems that include many transducers and media of propagation. The models of this category are simpler. In this category two models dominate: The first one was introduced by Mason (1948) and the second which known as KLM by Krimholtz, Leedom and Matthaei (1970) [1]. Both of these models are equivalent circuits and they are valid for a large range of operating conditions of a transducer. For example the KLM model can describe the behaviour of a piezoelectric transmitter with satisfactory accuracy when the transducer is operating either in air or in water. The basic characteristics of these two cases are transmission lines and non-real components such as negative capacitance. The transmission lines model the wave phenomena which are involved in the operation of the transducer. These phenomena are significant and can't be ignored. Transmission lines have generally transfer functions of infinite order because they host waves. The mathematics that are introduced due to the existence of these transmission lines and of the other elements of the equivalent circuits, make difficult or impossible the analytical solution of these circuits. The few mathematical formulas that can be derived are very complicated to be construable and useful. So these models are useful only for numerical simulation.

The second category also includes various simple analytical models. We sometimes happen to find the modelling of the behaviour of a transducer with a transfer function of second order with complex poles. These models are usually assumed and not developed or proven in all of the known cases.

The above models are well justified for studying the transducer's characteristics but are rather useless for the electronic systems designers. By contrast the electronic designers are interested to models developed on the data from measurements of electronic characteristics of the transducers. In the bibliography also we find cases where mainly becomes effort for the matching of the preamplifier section with an as possible resistive load (transmission line - sensor) [2], or for the matching between the generator of ultrasounds and the

transmission line [3], or for the matching of the impedance of the sensor with the transmission line. [4]. All the above cases concern operation of sensors in MHz frequencies and also they are not focused in the study of sensor as an electric equivalent of fig 1.

### 2. ANALYSIS OF THE MODEL

An approximation of the actual driving point impedance is used to derive the electrical characteristics of the transducer. The equivalent model is in most cases an electrical circuit of a capacitance  $C_0$  in parallel with a branch of three components in series (a resistance, a capacitance, and an inductance) called series – resistance etc. (fig. 1).

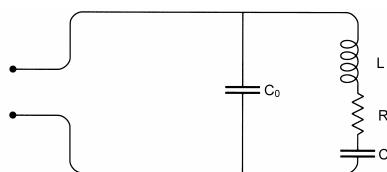


Fig. 1. The equivalent circuit

The impedance versus frequency of the transducer gives a lot of information about the characteristics of the transducer and can be used to find the component values of the equivalent electrical model.

Although the electrical equivalent looks very simple, the impedance is rather complex. Far away from the resonant frequency  $R$ ,  $C$ , and  $L$  have little influence and the impedance equals  $C_0$ . At the series resonant frequency the impedance is small and equal to the parallel circuit of  $R$  and  $C_0$ . Slightly above the resonant frequency, the series circuit  $R$ ,  $L$ ,  $C$  looks inductive and can start a parallel resonance with  $C_0$ . This causes a peak in the impedance curve.

The equivalent impedance is changing more than one order of magnitude during the resonance phenomenon (from 500Ohms to more than 5kOhms).

The respective values of the components appearing in this model may be estimated by electrical measurements only. The value of  $C_0$  may be estimated from the total impedance value in the frequency range well above the resonance frequency where  $Z_{total} = Z_{C_0}$ . In this case if only the characteristics of the driving circuit (voltage source) are known, then the capacitance  $C_0$  value may be estimated. Similarly the value of resistance  $R$  in the same model may be estimated by considering that it is equal to the overall circuit's series impedance at the resonance frequency. This figure may be also measured if we identify first the frequency values for the series and the parallel resonance. These two may be estimated by obtaining the impedance variation curve versus frequency. Then the value of the rest two components may be calculated by the corresponding equations [7], relating parallel and series resonance frequencies to the  $L$  and  $C$  values:

$$f_s = \frac{1}{2\pi\sqrt{LC}} \tag{1}$$

$$f_p = \frac{1}{2\pi\sqrt{L\frac{CC_0}{C+C_0}}} \tag{2}$$

### 3. INFLUENCE OF THE DRIVING CIRCUITS

In order to analyse the characteristics and operational response of the ultrasonic transducers we shall make a separate analysis for transmitting, receiving and coupled transducers.

#### 3.1. Simulation analysis of the equivalent circuit of the transmitting transducer.

The following figures refer to a transmitting transducer with:

- $f_s=39038\text{Hz}$ , bandwidth=1000Hz
- $f_p=41360\text{Hz}$ , bandwidth=1300Hz
- $R=0.558\text{ k}\Omega$ ,  $C=0.228\text{ nF}$ ,  $L=72.8\text{ mH}$ ,  $C_0=1.863\text{ nF}$

These values measured experimentally with the method described in the previous paragraph. The circuit of figure 2 is the equivalent circuit of the transmitter without modification elements.

Figure 3 represents the simulation of the series circuit and figure 4 the simulation of the overall circuit.

The data from this configuration analysis are:

- $f_s=39050\text{Hz}$ , bandwidth=1100Hz
- $f_p=41400\text{Hz}$ , bandwidth=1200Hz

Figure 5 shows the equivalent of the transmitter with  $L_1$ - $R_1$  modification elements, while figures 6 and 7 show the simulation of the series and parallel circuit respectively.

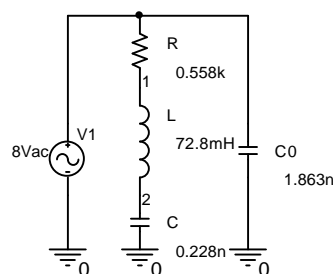


Fig. 2. The equivalent circuit of a transmitter without modification elements

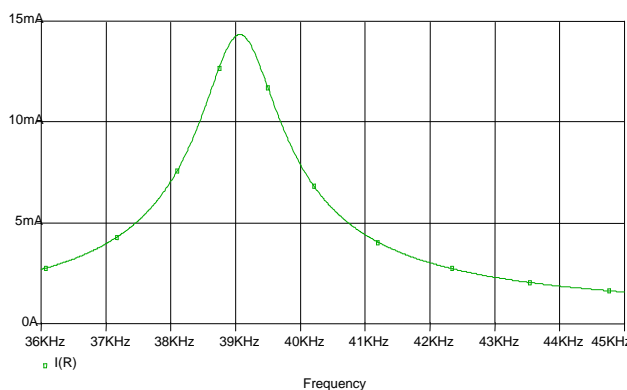


Fig. 3. Simulation of amplitude response of the series circuit of fig. 2

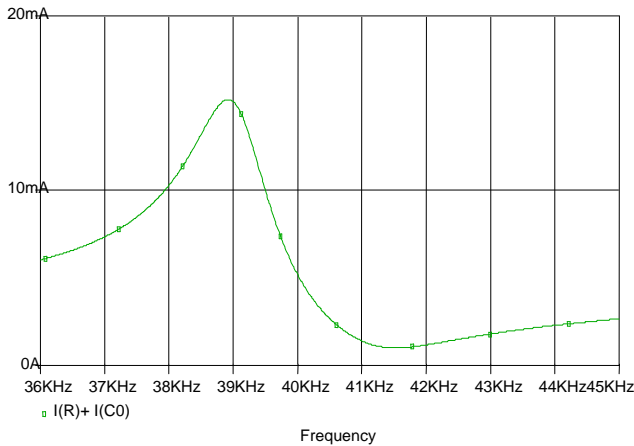


Fig. 4. Simulation of amplitude response of the overall circuit of fig. 2 where is distinctive the frequency of parallel resonance  $f_p$

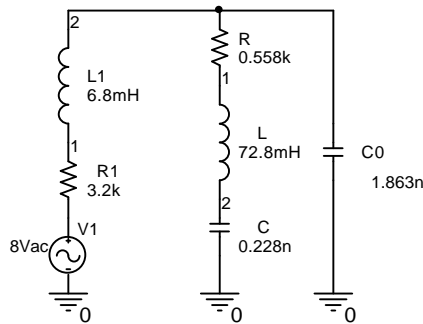


Fig. 5. The equivalent circuit of a transmitter with  $L_1$ - $R_1$  modification elements.

The data from this configuration analysis are:

- $f_s=41300\text{Hz}$ , bandwidth=4200Hz.
- $f_p=41400\text{Hz}$ , bandwidth=3750Hz

We can notice that there is a significant increase of the bandwidths in both resonant frequencies.

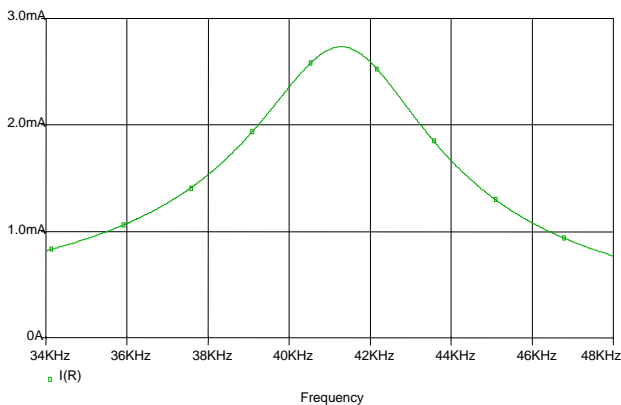


Fig. 6. Simulation of amplitude response of the series circuit of fig. 5

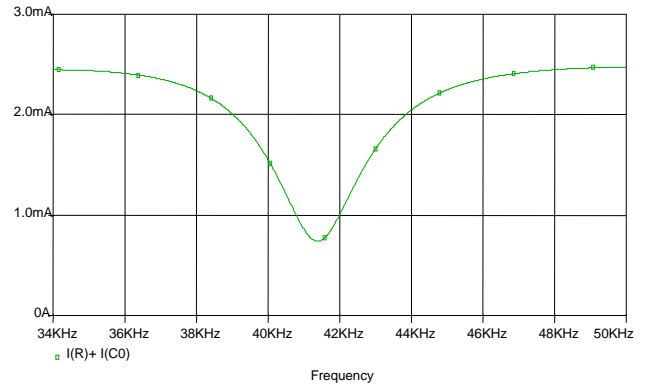


Fig. 7. Simulation of amplitude response of the parallel circuit of fig. 5

### 3.2. Simulation analysis of the equivalent circuit of the receiving transducer.

In this case a receiving transducer with the following characteristics has been simulated:

- $f_s=38510\text{Hz}$ , bandwidth=960Hz
- $f_p=40520\text{Hz}$ , bandwidth=920Hz
- $R=0.45\text{ k}\Omega$ ,  $C=0.198\text{nF}$ ,  $L=86.3\text{mH}$ ,  $C_0=1.848\text{nF}$ .

In the same way the circuit of figure 8 is the equivalent circuit of the transmitter without modification elements, while figure 9 represents the simulation of this series circuit.

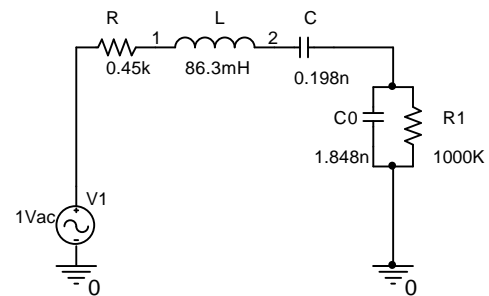


Fig. 8. The equivalent circuit of a receiver, without modification elements.

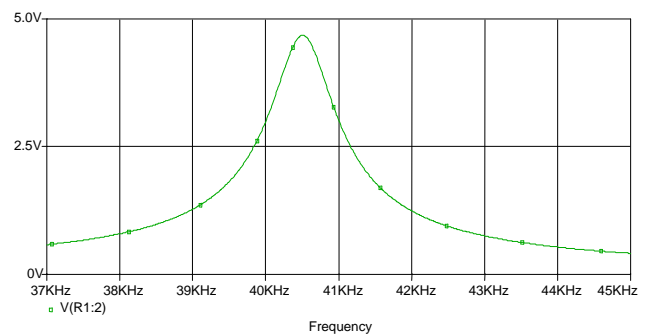


Fig. 9. Simulation of amplitude response of the circuit of fig. 8

A significant notice in this case is that the resonance frequency of this circuit is the same as the frequency  $f_p$  of the parallel branch of the equivalent circuit of fig. 1. In fact the resonant frequency of circuit of fig 8 (which is a series

circuit with L and the series combination of C and C<sub>0</sub>) is given by:

$$f_s = \frac{1}{2p \sqrt{L \frac{CC_0}{C+C_0}}} \quad (3)$$

which coincides with (2).

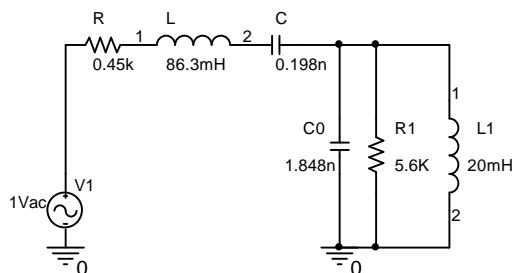


Fig. 10. The equivalent circuit of a receiver with L<sub>1</sub>-R<sub>1</sub> modification elements

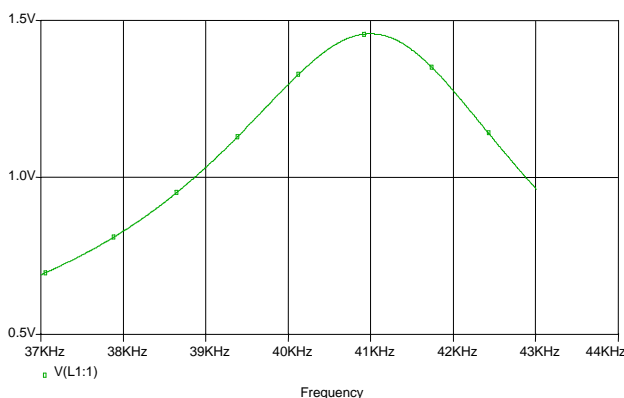


Fig.11. Simulation of amplitude response of the circuit of fig. 10

So the resonance frequency of an equivalent circuit for a receiving transducer is the same as f<sub>p</sub> of the general equivalent of fig 1. In this case f<sub>s</sub>=40500Hz, bandwidth=900Hz.

Figure 10 shows the equivalent of the receiver with L<sub>1</sub>-R<sub>1</sub> modification elements, while figure 11 shows the simulation of this circuit respectively. The resonance frequency of this equivalent is 41000Hz, while the (expanded) bandwidth is 3900Hz.

### 3.3. Experimental analysis of coupled transducers.

In this part the data analysis of coupled transducers (transmitter - air - receiver) is presented. Experimental measurements were performed for a pair of ultrasonic sensors with an automated system designed for the evaluation of ultrasonic transducers operating in the range of 40 KHz. This instrumentation configuration has been developed with the aim to perform automated tests and measurements of the values of important parameters of these

transducers [8]. The basic feature of this system includes the fast and accurate measurement of the frequency and amplitude which are performed in each period of the received signal. Figure 12 shows the amplitude response of a coupled pair of transducers (the same transducers which studied as discrete) without modification elements.

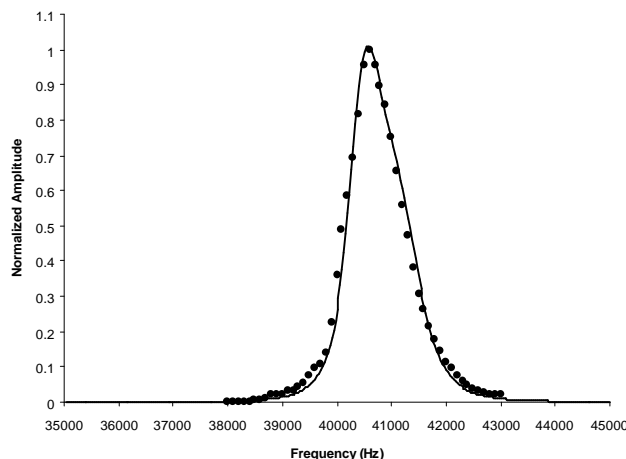


Fig. 12. Amplitude response of a coupled pair of transducers without modification elements.

In this figure dotted curve represents experimental data, while continuous curve represents theoretical data. For this pair the amplitude response was measured as a function of frequency. The transmitting signal was a sweep ultrasonic signal from 37KHz to 45KHz, with a step of 100Hz and step duration of 100 periods. Afterwards these sets of values (amplitude, frequency) are imported in a fitting process software based on the trial and error technique, which developed especially for this purpose.

The program calculates the values of the four parameters: f<sub>0T</sub>, BW<sub>T</sub>, f<sub>0R</sub>, BW<sub>R</sub>, in order that the curve H(s) approaches as much as possible in the experimental data. The experimental data of the frequency response of the pair of the transducers are a total number of points in the form of (f<sub>i</sub>, a<sub>i</sub>) with f<sub>i</sub> the frequency and a<sub>i</sub> the norm of H(s), namely the ratio of the amplitude of the output to the amplitude of the input.

The program works as follows:

- It is given in the program a range of values for each one of the parameters f<sub>0T</sub>, BW<sub>T</sub>, f<sub>0R</sub>, BW<sub>R</sub>.
- The program sweeps this range, finds the total number of values of the parameters f<sub>0T</sub>, BW<sub>T</sub>, f<sub>0R</sub>, BW<sub>R</sub>, and gives the most optimal approach in the experimental data. The criterion of most optimal approach is the minimisation of the sum:

$$s = \sum_i^N \left| 1 - \frac{\frac{|H(f_i)|^2}{a_i^2}}{\frac{1}{N} \sum_i^N \frac{|H(f_i)|^2}{a_i^2}} \right| a_i^2 \quad (4)$$

This criterion tries to approach in shape the theoretical curve  $|H(s)|^2$  in the experimental points  $a_i^2$ , giving more weight in the points with large  $a_i^2$  and least weight in the points with small  $a_i^2$ .

The objective of this procedure is to evaluate how close the theoretical analysis to experimental behaviour is by estimating the approximation of experimental data with a continuous function. The expression of this function is taken for granted (based on theoretical analysis) and is the expression of the transfer function of the system transmitter-receiver:

$$H(s) = k \frac{s}{s^2 + 2pBW_T s + (2pf_{0T})^2} \frac{s}{s^2 + 2pBW_R s + (2pf_{0R})^2} \quad (5)$$

For a successful approximation this routine searches for the best values of the four parameters which appear in the above expression and are:  $f_{0T}$  (resonance frequency of the transmitter),  $BW_T$  (bandwidth of the transmitter),  $f_{0R}$  (resonance frequency of the receiver), and  $BW_R$  (bandwidth of the receiver).

These best values which are the results of the software routine give the best approximation, according to the approximation criterion used for their selection.

For the pair of fig. 12 the fitting process gave values of the transducer parameters:  $f_{0T} = 41181.25\text{Hz}$ ,  $BW_T = 1265.625\text{Hz}$ ,  $f_{0R} = 40356.25\text{Hz}$ ,  $BW_R = 1046.875\text{Hz}$ .

Figure 13 shows the data for a coupled pair of transducers, where the receiver is in natural response, while the transmitter is with  $L_1$ - $R_1$  modification elements same as in fig. 5. In this configuration, data give resonance frequency of the receiver 40800Hz and bandwidth 950Hz.

The case of fig. 14 refers to a pair of coupled transducers where the transmitter is in natural response, while the receiver is with  $L_1$ - $R_1$  modification elements same as in fig. 10.

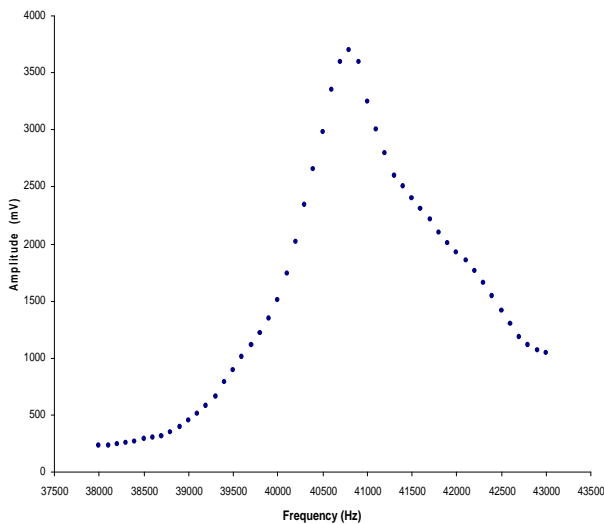


Fig. 13. Amplitude response of a coupled pair of transducers with modification elements on the transmitting transducer.

In this figure two areas are shown, one of series resonance

with  $f_s=39500\text{Hz}$  and bandwidth 1100Hz and the other of parallel resonance with  $f_p=41550\text{Hz}$  and bandwidth 1200Hz.

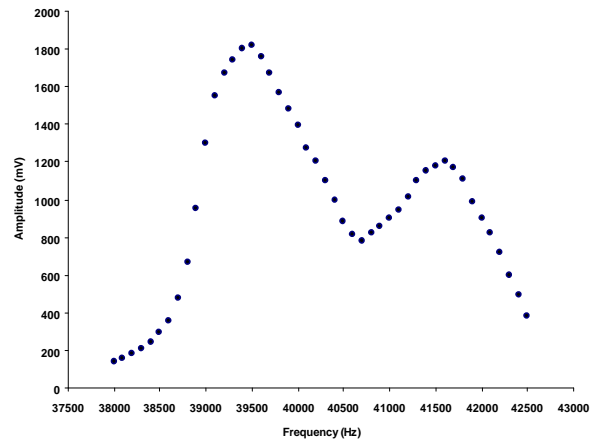


Fig. 14. Amplitude response of a coupled pair of transducers with modification elements on the receiving transducer.

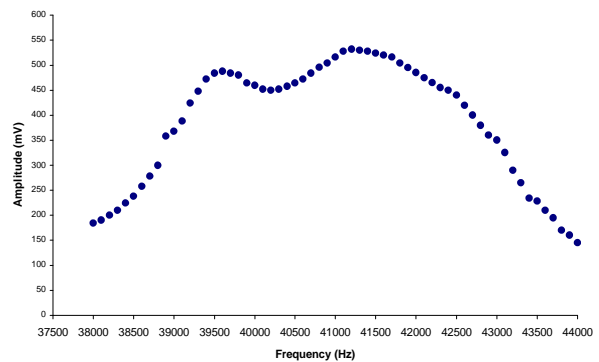


Fig. 15. Amplitude response of a coupled pair of transducers with modification elements on both transducers.

Last case is this one with modification elements on both transducers, as fig. 15 shows. The values of the modification elements  $L_1 - R_1$  are the same as in fig. 5 and 10 for the transmitter and the receiver respectively. Here the increased bandwidth is 3850Hz.

### 3.3. Data analysis of measurements.

The data analysis of the transmitting and receiving transducers for the series and parallel resonance (frequencies and bandwidths) and for different type of measurements are presented in the following.

#### 1. Transmitting transducer.

a) Series resonance. The data from: the experimental measurements of the discrete transmitting transducer of figure 1, the simulation of the discrete transducer of figures 2,3 and the experimental measurements of the coupled transducers of figure 14 gave a mean value of series resonant frequency of  $\bar{f}_s = 39193\text{Hz}$  with a % deviation

from  $\overline{f_s}$  in the range of 0.37% to 0.78%. Also the mean value of bandwidth found to be  $\overline{BW_s} = 1066.67\text{Hz}$ , while the % deviation from  $\overline{BW_s}$  ranged between 3.12% and 6.25%.

b) Parallel resonance. In this case the collected data from: the experimental measurements of the discrete transmitting transducer of figure 1, the simulation of the discrete transducer of figures 2,4, the experimental measurements of the coupled transducers of figure 14 and the experimental measurements of the coupled transducers with fitting process of figure 12 gave a mean value of parallel resonant frequency of  $\overline{f_p} = 41372.75\text{Hz}$  with a % deviation from  $\overline{f_p}$  in the range of 0.031% to 0.46%. Also the mean value of bandwidth found to be  $\overline{BW_p} = 1241.25\text{Hz}$ , while the % deviation from  $\overline{BW_p}$  ranged between 1.93% and 4.75%.

## 2. Receiving transducer.

a) Series resonance. In this case the data were only from the experimental measurements of the discrete receiving transducer of figure 1. These data gave a series resonant frequency  $f_s = 38510\text{Hz}$  and bandwidth  $BW_s = 960\text{Hz}$ .

b) Parallel resonance. In the same way as for the transmitting transducer the collected data were from: the experimental measurements of the discrete transmitting transducer of figure 1, the simulation of the discrete transducer of figures 8,9, the experimental measurements of the coupled transducers of figure 13 and the experimental measurements of the coupled transducers with fitting process of figure 12. These data gave a mean value of parallel resonant frequency of  $\overline{f_p} = 40544\text{Hz}$  with a % deviation from  $\overline{f_p}$  in the range of 0.059% to 0.63%. Also the mean value of bandwidth found to be  $\overline{BW_p} = 954\text{Hz}$ , while the % deviation from  $\overline{BW_p}$  ranged between 0.42% and 9.64%.

Finally the comparison of figures 10, 11, 15, verifies the coincidence of the values of bandwidths of the receiving transducer from the simulation of the discrete transducer with  $L_1$ - $R_1$  modification elements on the one hand and from the experimental measurements of the coupled transducers with  $L_1$ - $R_1$  modification elements on both transducers on the other hand. These values are 3900Hz and 3850Hz respectively.

## 4. CONCLUSION

The influence of the driving circuits on the resonant characteristics of airborne ultrasonic transducers has been presented. The study proved that it is possible to change these characteristics (for example resonance frequency and bandwidth) with a proper selection of the discrete elements ( $R_1$ - $L_1$ ), according to our measurement technique demands. On most applications of ultrasonic systems, the overall performance depends on the characteristics of operation of sensors, mainly on the frequency response and their sensitivity.

The acoustic response of such configurations depends drastically on the characteristics of the driving circuits,

which provide the electric connection between the sensors and the electronic system. The electronic elements of the input of the system affect on the width and the shape of the transmitted ultrasound pulses, leading thus to a situation where a different approach will be supported, depending on the specific application.

In the bibliography were met cases where mainly becomes effort of matching of sensors with the transmission line of the transmitting or receiving signal.

In this paper the influence of R-L adaptive elements on the operation of the transmitting and receiving ultrasound transducers has been analyzed. First a method for the estimation of R, L, C,  $C_0$ ,  $f_s$ ,  $f_p$ ,  $BW_s$ ,  $BW_p$  of the electrical equivalent circuit was described, then simulated and experimental data for different cases of discrete and coupled transducers were analyzed and finally the overall evaluation of the data was given.

## REFERENCES

- [1] G.S. Kino, *Acoustic Waves: Devices, Imaging, and Analog Signal Processing*. Englewood Cliffs, New Jersey: Prentice-Hall, 1987.
- [2] Ron McKeighen, Ph.D., "Influence of Pulse Drive Shape and Tuning on the Broadband Response of a Transducer", *Proc IEEE Ultrasonics Symposium*, Vol 2, pp. 1637-1642
- [3] Lorenzo Capineri, Member, IEEE, Leonardo Masotti, Marco Rinieri, and Santina Rocchi "Ultrasonic Transducer as a Black-Box: Equivalent Circuit Synthesis and Matching Network Design", *IEEE Transactions on Ultrasonics, Ferroelectrics, and Frequency Control*, Vol.40, No. 6, November 1993, pp. 694-702.
- [4] Antonio Ramos, Jose L. San Emeterio, Member, IEEE, and Pedro T. Sanz, "Improvement in Transient Piezoelectric Response of NDE Transceivers Using Selective Damping and Tuning Networks" *IEEE Transactions on Ultrasonics, Ferroelectrics, and Control*, Vol.47, No4, July 2000, pp.826-835.
- [5] Theodore L. Rhyne, Member, IEE "Computer Optimization of Transducer Transfer Functions Using Constraints on Bandwidth, Ripple, and Loss", *IEEE Transactions on Ultrasonics, Ferroelectrics, and Frequency Control*, Vol. 43, No. 6, November 1996, pp. 1136-1149.
- [6] F.J. Arnold, S.S. Muhlen, "The resonance frequencies on mechanically pre-stressed ultrasonic piezotransducers" *Elsevier Ultrasonics Vol. 39 (2001) pp. 1-5*
- [7] *Piezoelectric Ceramic Sensors (Piezotite)*, Murata Manufacturing Co., Ltd., Cat.No.P19E-6.
- [8] Ch. Papageorgiou, C. Kosmatopoulos and Th. Laopoulos, "Automated characterization and calibration of ultrasonic transducers", 9<sup>th</sup> Mediterranean Electrotechnical Conference (MELECON '98), Tel-Aviv, Israel 1998.

Chris Papageorgiou, Electronics Lab. Physics Dept., Aristotle University of Thessaloniki, Thessaloniki, 54124, Greece, phone: +302310938039, fax: +302310998018, e-mail: papageorgiou@physics.auth.gr.

Theodore Laopoulos, Electronics Lab. Physics Dept., Aristotle University of Thessaloniki, Thessaloniki, 54124, Greece, phone: +302310998215, fax: +302310998018, e-mail: laopoulos@physics.auth.gr.